Journal of Biomolecular NMR, **23:** 47–55, 2002.
KLUWER/ESCOM

Angular dependence of $^1J(N_i,C_{\alpha i})$ and $^2J(N_i,C_{\alpha(i-1)})$ coupling constants measured in J-modulated HSQCs

Julia Wirmer & Harald Schwalbe*
Department of Chemistry and MIT/Harvard Center for Magnetic Resonance at the Francis Bitter Magnet Laboratory, Massachusetts Institute of Technology, 77 Massachusetts Avenue, Cambridge, MA 02139, U.S.A.

Received 19 February 2002; Accepted 20 February 2002

Key words: ^{1}J and ^{2}J scalar couplings, Karplus-equation, NMR, random coil, ubiquitin

Abstract

A new method to measure $^1J(N_i,C_{\alpha i})$ and $^2J(N_i,C_{\alpha(i-1)})$ coupling constants in proteins based on a J-modulated sensitivity enhanced HSQC was introduced. Coupling constants were measured in the denatured and in the native state of ubiquitin and found to depend on the conformation of the protein backbone. Using a combined data set of experimental coupling constants from ubiquitin and staphylococcal nuclease (Delaglio et al., 1991), the angular dependence of the coupling constants on the backbone angles ψ and ϕ was investigated. It was found that the size of $^2J(N_i,C_{\alpha(i-1)})$ correlates strongly with the backbone conformation, while only a weak conformational dependence on the size of $^1J(N_i,C_{\alpha i})$ coupling constants was observed. Coupling constants in the denatured state of ubiquitin were uniform along the sequence of the protein and not dependent on a given residue type. Furthermore it was shown that the observed coupling constants were in good agreement with predicted coupling constants using a simple model for the random coil.

The dependence of the size of ^{3}J coupling constants on the intervening torsion angle is widely used to determine the local conformation and conformational equilibria by NMR spectroscopy (Bystrov, 1976). In contrast, the conformational dependence of ^{1}J (Mierke et al., 1992; Juranić and Macura, 2001) and ^{2}J coupling constants is less well characterized.

A number of triple resonance experiments such as the HNCA experiment (Kay et al., 1991) rely on magnetization transfer via $^1J(N_i,C_{\alpha i})$ and $^2J(N_i,C_{\alpha(i-1)})$ couplings. These couplings are in principle readily accessible, but few reports have investigated the size of $^1J(N_i,C_{\alpha i})$ and $^2J(N_i,C_{\alpha(i-1)})$ coupling constants and their dependence on sequence and structure. In peptides, values of $^1J(N_i,C_{\alpha i}) \sim 11$ Hz and $^2J(N_i,C_{\alpha(i-1)}) \sim 7$ Hz have been reported (Bystrov, 1976). In staphylococcal nuclease, Delaglio et al. (1991) have measured $^1J(N_i,C_{\alpha i})$ and $^2J(N_i,C_{\alpha(i-1)})$ coupling constants and observed their dependence on secondary structure. Edison et al. (1994a,b) have derived a parametrization for $^1J(N_i,C_{\alpha i})$ and $^2J(N_i,C_{\alpha(i-1)})$ coupling constants from *ab-initio* calculations as a function of the angles ϕ and ψ. The experimental data of Delaglio et al. (1991) were found to correlate well with the predictions from the *ab-initio* calculations. Further experimental data on ubiquitin were provided from the groups of A. Annila (Permi and Annila, 2000; Permi et al., 2000) and I. Kilpeläinen (Heikkinenen et al., 2001).

In this report, $^1J(N_i,C_{\alpha i})$ and $^2J(N_i,C_{\alpha(i-1)})$ coupling constants have been measured using J-modulated HSQCs (Neri et al., 1990; Billeter et al., 1992; Vuister et al., 1993; Kuboniwa et al., 1994; Tjandra et al., 1996; Tjandra and Bax, 1997). We have chosen these quantitative experiments (Bax et al., 1994) since they are easy to implement and to automate and do not require prior knowledge of coupling constants for optimal unwanted peak suppression.

*To whom correspondence should be addressed. Present address: Center for Biological Magnetic Resonance, Institut für Organische Chemie, Johann Wolfgang Goethe-Universität, Marie-Curie-Str. 11, 60439 Frankfurt/M., Germany. E-mail: schwalbe@nmr.uni_frankfurt.de

The conformational dependence of the coupling constants has been analyzed. In addition, the sequence dependence of the coupling constants has been investigated by measuring the coupling constants both in denatured ubiquitin (8 M urea, pH 2, T = 298 K) as well as in native ubiquitin (30 mM sodium acetate buffer, pH 4.7, T = 298 K). In agreement with previous data in the literature, we found a dependence of the $^1J(N_i,C_{\alpha i})$ and $^2J(N_i,C_{\alpha(i-1)})$ coupling constants on the conformation of the protein backbone. Furthermore, uniform coupling constants were found in the unfolded state of ubiquitin. These findings suggest that the coupling constants are independent of the amino acid sequence and type. Based on the data by Delaglio et al. (1991) for staphylococcal nuclease and the data measured in this report for ubiquitin, improved Karplus-type relations are derived. It is found that $^1J(N_i,C_{\alpha i})$ show a weak dependence on ψ and that $^2J(N_i,C_{\alpha(i-1)})$ depend on both angles $\phi_{(i-1)}$ and $\psi_{(i-1)}$.

Pulse sequence description

Figure 1 shows the pulse sequence for the measurement of $^1J(N_i,C_{\alpha i})$ and $^2J(N_i,C_{\alpha(i-1)})$ coupling constants. The experiment is based on a J-modulated sensitivity enhanced ^1H,^{15}N-HSQC (Neri et al., 1990; Billeter et al., 1992; Vuister et al., 1993; Kuboniwa et al., 1994; Tjandra, 1996; Tjandra and Bax, 1997): $^1J(N_i,C_{\alpha i})$ and $^2J(N_i,C_{\alpha(i-1)})$ coupling constants evolve during a delay τ before the evolution of the nitrogen chemical shift during t_1. Variation of τ in a series of experiments and fitting the signal intensities can therefore be used to determine the coupling constants. Due to the limited chemical shift dispersion in the C_α region, the pulse sequence cannot be applied to measure couplings for residues that have either serines, threonines or glycines as the nearest neighbor, due to chemical shift overlap.

Experimental section

A sample of uniformly ^{13}C,^{15}N labeled human ubiquitin (VLI Research, Malvern, PA) was used without further purification. 5 mg were dissolved in 300 µl of 90% H_2O, 10% D_2O containing 30 mM sodium acetate buffer, pH 4.7 for folded ubiquitin; and 5mg were dissolved in 300 µl of 90% H_2O, 10% D_2O containing 8 M urea, pH 2 for denatured ubiquitin. All spectra were recorded on a four-channel Bruker DRX600 spectrometer equipped with an actively shielded z-gradient probe at a temperature of 298K. Sequential assignments of the denatured (Peti et al., 2001) and native (Wang et al., 1995) ubiquitin were found to be valid using HNCA spectra.

Pulsed field gradients were used for coherence order selective coherence transfer, making use of sensitivity enhancement for the J-modulated HSQC experiment. 64 complex points with an acquisition time of 65.536 ms for ^{15}N (ω_1) and 2048 complex points with an acquisition time of 256 ms were recorded for $^1H^N$ at a frequency of 600 MHz.

Spectra were processed with Xwinnmr (Bruker, Karlsruhe) and analyzed using the program Felix 98.0 (Biosym/MSI, San Diego, CA). Data sets were zerofilled and Fourier transformed retaining only the $^1H^N$ region of the spectra. Apodization with a 90° shifted sinebell window function was used. The final 2D matrices consist of 2048 × 1024 real points.

Determination of $^1J(N_i,C_{\alpha i})$ and $^2J(N_i,C_{\alpha(i-1)})$ coupling constants

A series of experiments with τ = 20 µs – 150 ms was collected for native (18 points) and for denatured ubiquitin (14 points). Measured peak intensities were fitted to:

$$I^{exp} = A\cos(\pi^1 J\tau)\cos(\pi^2 J\tau)e^{-\tau/T_2^*}, \quad (1)$$

where I^{exp} is the experimental peak height intensiy, $^1J = {}^1J(N_i,C_{\alpha i})$, $^2J = {}^2J(N_i,C_{\alpha(i-1)})$, A is a fitted amplitude factor and T_2^* is the transverse relaxation rate for this $\tau/2 - \pi - \tau/2$ echo sequence (see Figure 1). Figure 2 shows an example of the curve fit for the peaks of Arg42 and Glu51. The intensity modulation could reliably be fitted.

To decrease the number of fitting parameters, T_2^* values were determined in an independent series of experiments for native ubiquitin by omitting the C_α selective pulse in the pulse sequence shown in Figure 1. T_2^* values were obtained by fitting peak intensities to a mono-exponential decay. Comparison of the values for T_2^* derived from fitting to equation 1 with the independently determined T_2^* revealed that the fitted and the independent T_2^* values agree within the error margins. Therefore, in the case of denatured ubiquitin, T_2^* values were not independently measured.

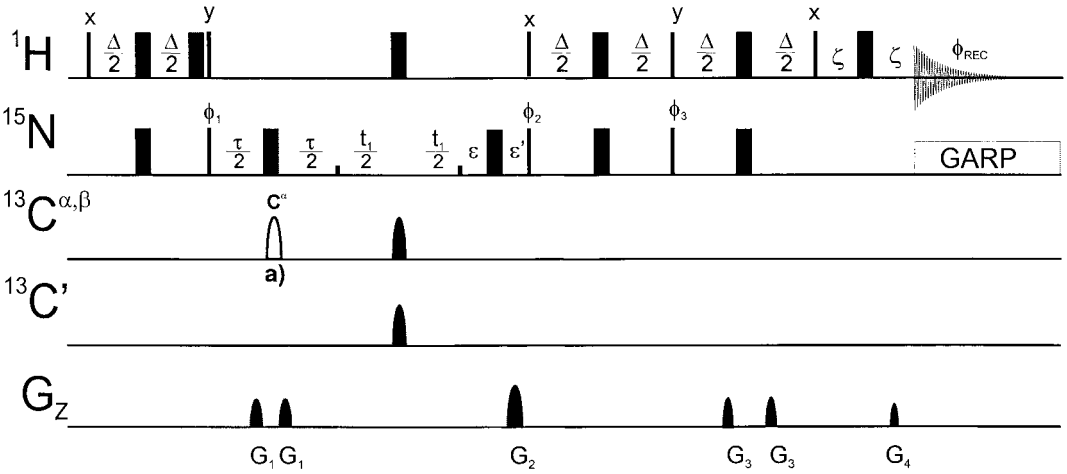

Figure 1. Pulse scheme for measurement of $^1J(N_i,C_{\alpha i})$ and $^2J(N_i,C_{\alpha(i-1)})$ coupling constants: Carrier positions in the present work were 4.707 ppm for ^{1}H (H_2O on resonance), 178.221 ppm for $^{13}C'$, 58.678 ppm for $^{13}C_\alpha$ and 116.77 ppm for ^{15}N. A trim pulse of 1ms was applied at high proton pulse power, high power proton pulses were applied with a field strength of 34.7 kHz. ^{15}N decoupling during acquisition employed a 2.3 kHz GARP (Shaka et al., 1985) field, while high power ^{15}N pulses were applied with a field strength of 6.6 kHz. Narrow and wide pulses denote 90° and 180° flip angles, respectively and unless indicated, the phase is x. Carbon 180° pulses were implemented as phase modulated G3 inversion pulses (Emsley and Bodenhausen, 1990) of durations 1000 μs for the selective C_α inversion pulse in the middle of τ and 512μs for decoupling inversion pulses. Delay durations: $\Delta = 5.5$ ms, $\tau = 20$ μs–150 ms, ε and ε′ were adjusted to avoid chemical shift evolution for $t_1 = 0$, $\zeta = 1.507$ ms. Phase cycling: $\phi_1 = x, -x, \phi_2 = x, x, -x, -x, \phi_3 = -y, -y, y, y, \phi_{rec} = x, -x, -x, x$. For each t_1 value, echo- and antiecho coherences were obtained by recording data sets in which the phase ϕ_3 and Gradient G_2 were inverted. Sine shaped gradient durations and amplitudes were: $G_1 = 0.5$ ms (20 G/cm); $G_2 = 1$ ms (40 G/cm); $G_3 = 0.5$ ms (15 G/cm); $G_4 = 1$ ms (4.05 G/cm). Pulse scheme for the determination of T_2^*, omitting the selective C_α pulse (labeled with (a)) in the middle of τ.

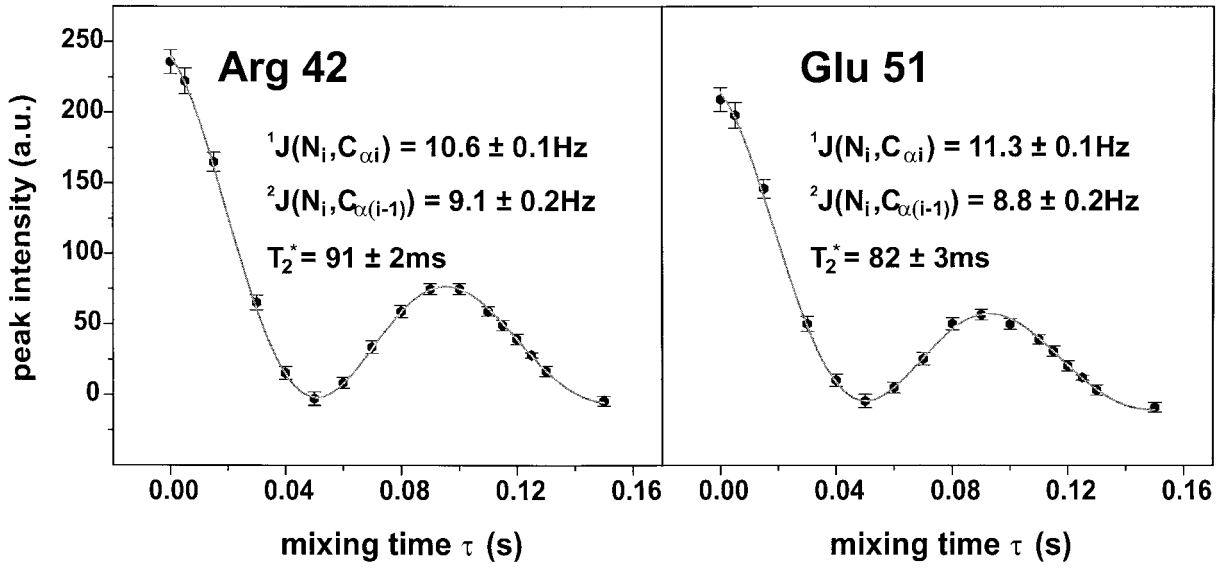

Figure 2. Experimental peak intensities (black diamonds) and fitting the equation $I = A\cos(\pi^1 J\tau)\cos(\pi^2 J\tau)e^{-\tau/T_2^*}$ to them (grey line) for the cross peaks of Arg 42 and Glu 51 in folded ubiquitin. Error bars for the peak intensities were deducted from the standard deviation of 15 noise peaks in each spectrum. The quality of the fit is $R^2 = 0.9993$ for Arg 42 and $R^2 = 0.9986$ for Glu 51. Fitting was performed using the program Origin. Examples shown here were chosen, for a comparison with the values with coupling constants measured by Heikkinenen et al. (2001).

Application to ubiquitin

$^1J(N_i,C_{\alpha i})$ and $^2J(N_i,C_{\alpha(i-1)})$ coupling constants were determined for 38 residues in folded ubiquitin. The following averaged values were found: $^1J(N_i,C_{\alpha i}) = 10.8 \pm 0.8$ Hz and $^2J(N_i,C_{\alpha(i-1)}) = 7.7 \pm 1.3$ Hz. The coupling constants measured in this report compare well (average observed deviation <0.3 Hz) with the selected set of 11 coupling constants published by Heikkinen et al. (2001) using a $^{13}C_\alpha$-coupled ^{15}N S^3E-HSQC experiment (Meissner et al., 1997).

In the J-modulated HSQC, a relatively large number of coupling constants could be determined since the experiment is not very sensitive to limited resolution. It was therefore possible to measure $^1J(N_i,C_{\alpha i}) = 10.9 \pm 0.2$ Hz and $^2J(N_i,C_{\alpha(i-1)}) = 8.0 \pm 0.3$ Hz in denatured ubiquitin for 28 residues as shown in Figure 3.

In the folded state, the size of $^1J(N_i,C_{\alpha i})$ and $^2J(N_i,C_{\alpha(i-1)})$ is correlated with the location of secondary structure elements in ubiquitin: Both $^1J(N_i,C_{\alpha i})$ and $^2J(N_i,C_{\alpha(i-1)})$ coupling constants are substantially larger in β-sheet regions ($^1J(N_i,C_{\alpha i}) = 11.2 \pm 0.5$ Hz and $^2J(N_i,C_{\alpha(i-1)}) = 8.4 \pm 0.7$ Hz) than in α-helices ($^1J(N_i,C_{\alpha i}) = 9.9 \pm 0.2$ Hz and $^2J(N_i,C_{\alpha(i-1)}) = 6.3 \pm 0.7$ Hz).

In contrast, the sizes of the coupling constants in denatured ubiquitin were found to be in between the values for α-helices and β-sheets ($^1J(N_i,C_{\alpha i}) = 10.9 \pm 0.2$ Hz and $^2J(N_i,C_{\alpha(i-1)}) = 8.0 \pm 0.3$ Hz) and, in addition, were found to be uniform along the sequence. The couplings, therefore, do not seem to be correlated with the primary sequence of the protein, and couplings do not show a marked dependence on the amino acid type.

Quantitative description of coupling constants in the folded state

$^1J(N_i,C_{\alpha i})$ and $^2J(N_i,C_{\alpha(i-1)})$ coupling constants for residues in staphylococcal nuclease (Delaglio et al., 1991) and in ubiquitin were analyzed in the following section. The structure dependence of the coupling constants in both proteins were in close agreement.

Analysis of $^1J(N_i, C_{\alpha i})$ coupling constants

The correlation of $^1J(N_i,C_{\alpha i})$ coupling constants on the torsion angles φ and ψ of ubiquitin (Cornilescu et al., 1998) and staphylococcal nuclease (Loll and Lattman, 1989) were investigated. A dependence of $^1J(N_i,C_{\alpha i})$ on φ alone could not be found: correlation to a Karplus equation ($f(\phi) = A + B\cos(\phi) + C\cos^2(\phi)$) leads to a correlation coefficient of $R = 0.56$ ($R^2 = 0.32$) with $A = 10.5792$, $B = -1.1616$ and $C = 0.3752$.

The correlation of $^1J(N_i,C_{\alpha i})$ with ψ is more pronounced: Figure 4A shows the curve resulting from a Karplus fit:

$$f(\psi) = A + B\cos(\psi) + C\cos^2(\psi). \quad (2)$$

The statistical significance of the fit is described by the correlation coefficient $R = 0.85$ ($R^2 = 0.72$); the coefficients are $A = 9.5098$, $B = -0.9799$ and $C = 1.7040$. The probability that this nonlinear correlation results from random uncertainties is negligible ($P < 10^{-4}$). To test whether a multi-dimensional model fits the data better than Equation 2, the 122 $^1J(N_i,C_{\alpha i})$ coupling constants measured for ubiquitin and for staphylococcal nuclease were fitted to a combined Karplus equation with dependencies on both φ and ψ:

$$\begin{aligned} f(\phi, \psi) &= A + B\cos(\phi) + C\cos^2(\phi) \\ &\quad + D\cos(\psi) + E\cos^2(\psi) \end{aligned} \quad (3)$$

defining a surface with coefficients $A = 9.5456$, $B = -0.1923$, $C = 0.0376$, $D = -0.9093$ and $E = 1.6250$. The correlation coefficient $R = 0.86$ ($R^2 = 0.73$) is slightly better than the one for Equation 2. Again, the probability that this correlation occurs by chance is negligible ($P < 10^{-4}$).

Following Hennig et al. (2000), $F-$statistics were used to test whether multi-dimensional models with more adjustable parameters represent the experimental data better (Bevington, 1969):

$$F = \nu_2(\chi_1 - \chi_2)/(\nu_1 - \nu_2)\chi_2. \quad (4)$$

In this equation, ν are the statistical degrees of freedom for a certain model $\nu = N - n$ (N = number of data points and n = numbers of parameters in the fit, $n_2 > n_1$), and χ = sum of squared errors between the experimental and the predicted parameters of the fit. Large values for F indicate a significant improvement of the fit as opposed to random statistical reduction of the χ value due to the incorporation of additional parameters. Critical values for an exact F-distribution $F_{0.01,N1,N2}$ ($N1 = n_2 - n_1$, $N2 = N - n_2$) can be used

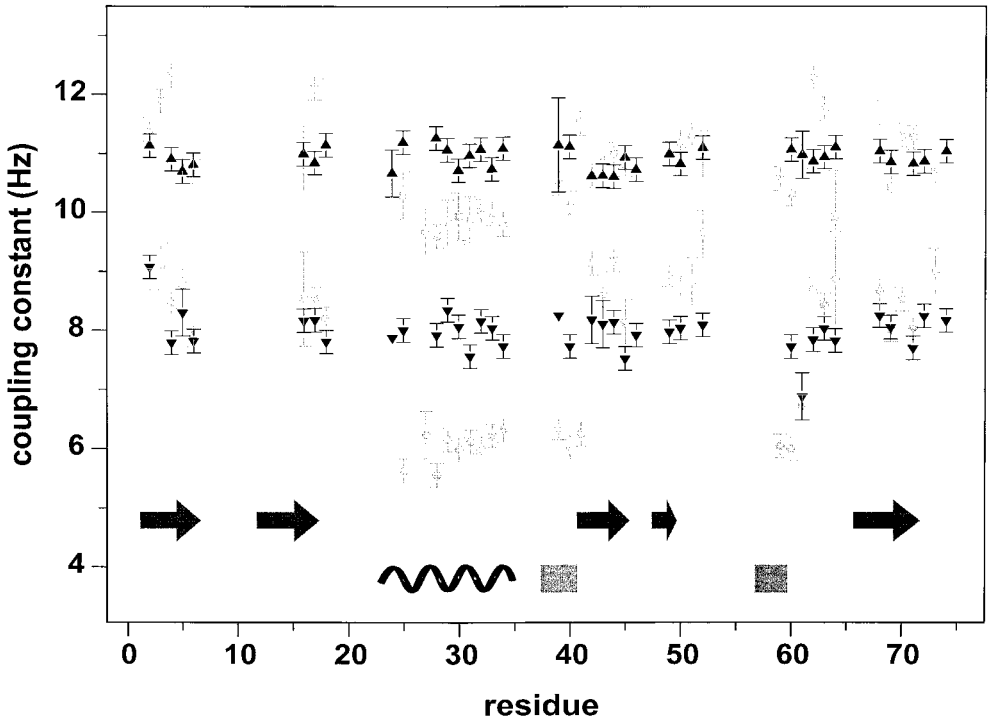

Figure 3. Correlation of $^{1}J(N_i,C_{\alpha i})$ and $^{2}J(N_i,C_{\alpha(i-1)})$ coupling constants of folded and denatured ubiquitin with the residue. Grey squares $^{1}J(N_i,C_{\alpha i})$ and grey circles $^{2}J(N_i,C_{\alpha(i-1)})$ coupling constants in folded ubiquitin; black triangles $^{1}J(N_i,C_{\alpha i})$ and $^{2}J(N_i,C_{\alpha(i-1)})$ coupling constants in denatured ubiquitin. Secondary structures as determined by the algorithm implemented in MOLMOL (Konradi et al., 1996) are also shown (arrow: β-sheets, helix: α-helix, grey bar: 3_{10}-helix). Error bars are according to the deviations given in the fit (see Figure 2).

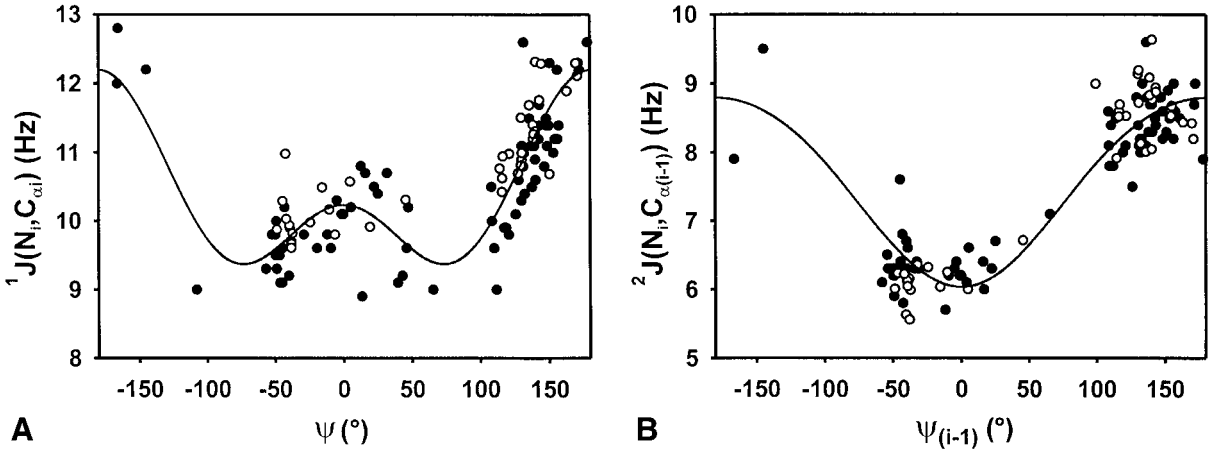

Figure 4. (A) $^{1}J(N_i,C_{\alpha i})$ coupling constants for residues in folded ubiquitin (open circles) and folded staphylococcal nuclease, (Delaglio et al., 1991) (filled circles) as a function of ψ torsion angles. The correlation coefficient R for the least squares Karplus fit $f(\psi) = A + B\cos(\psi) + C\cos^2(\psi)$ is 0.85. Coefficients are A = 9.5098, B = −0.9799 and C = 1.7040. (B) $^{2}J(N_i,C_{\alpha(i-1)})$ coupling constants of folded ubiquitin (open circles) and folded staphylococcal nuclease (Delaglio et al., 1991) (filled circles) as a function of $\psi_{(i-1)}$ torsion angles. The statistical significance of the Karplus relation between $\psi_{(i-1)}$ and $^{2}J(N_i,C_{\alpha(i-1)})$, $f(\psi_{(i-1)}) = A + B\cos(\psi_{(i-1)}) + C\cos^2(\psi_{(i-1)})$ is described by R = 0.91. The coefficients for the Karplus equation are A = 7.6213, B = −1.3791 and C = −0.2067.

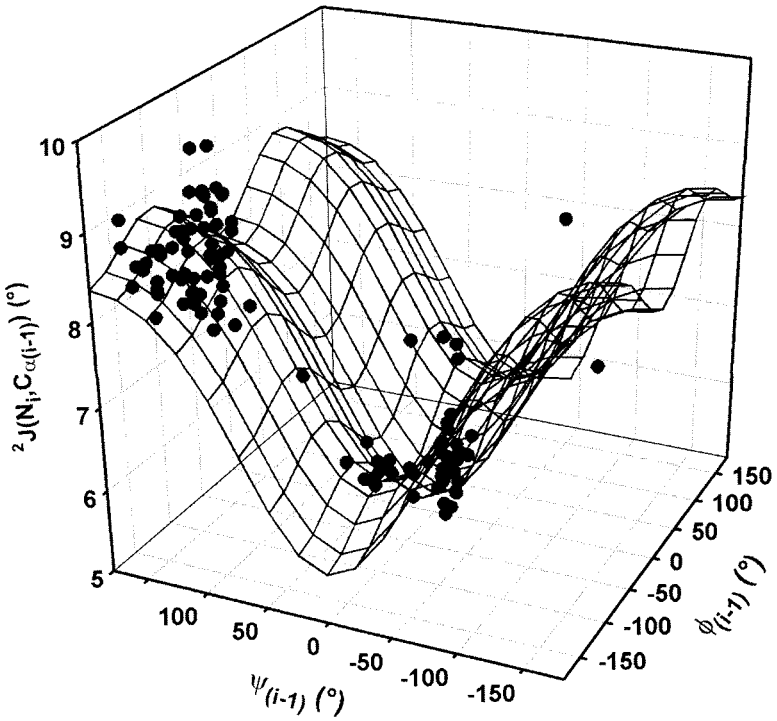

Figure 5. $^2J(N_i,C_{\alpha(i-1)})$ coupling constants of residues of folded ubiquitin and folded staphylococcal nuclease (Delaglio et al., 1991) as a function of neighboring $\phi_{(i-1)}$ and $\psi_{(i-1)}$ torsion angles. The experimental coupling constant values were fitted to the five parameter combined Karplus Equation 3: $f(\phi_{(i-1)}, \psi_{(i-1)}) = A + B\cos(\phi_{(i-1)}) + C\cos^2(\phi_{(i-1)}) + D\cos(\psi_{(i-1)}) + E\cos^2(\psi_{(i-1)})$, giving rise to the depicted surface. The correlation coefficient R for the least square fit is 0.94, the coefficients are A = 7.8163, B = −0.1717, C = −0.6408, D = −1.3892, E = −0.3709.

to evaluate the calculated F-value (Bronstein and Semendjajew, 1989).

The calculated value, $F = 1.40$, is smaller than the corresponding critical value $F_{0.01,2,117} \approx 4.80$ (the tabulated F value for N = 128 and N = 103 are $F_{0.01,2,125} = 4.78$, $F_{0.01,2,100} = 4.82$, respectively). The related coefficients B and C in Equation 3 do therefore not statistically deviate from zero and must not be included in the model.

However, Edison et al. (1994 a,b) predicted $^1J(N_i,C_{\alpha i})$ using *ab-initio* calculations and fitted them to a second order Fourier analysis (M = N = 2) in terms of ϕ and ψ:

$$\begin{aligned} f(\phi, \psi) \;=\; & \sum_{i}^{M}\sum_{j}^{N} \{\cos(i\phi)\cos(j\psi) \\ & + \cos(i\phi)\sin(j\psi) \\ & + \sin(i\phi)\cos(j\psi) \\ & + \sin(i\phi)\sin(j\psi)\}\,. \end{aligned} \tag{5}$$

The coupling constants derived from Equation 5 were correlated with experimental coupling constants from staphylococcal nuclease. The least square minimization of the linear correlation lead to a correlation coefficient of R = 0.87 ($R^2 = 0.75$). The correlation of the experimental $^1J(N_i,C_{\alpha i})$ of ubiquitin and staphylococcal nuclease with the predicted coupling constants from Equation 5 yielded a correlation coefficient of R = 0.81 ($R^2 = 0.66$). Using F-statistics to compare the models described by Equation 5 (25 coefficients) and the ϕ independent Karplus equation with 3 coefficients (Equation 2) show that Equation 2 is a statistically better model for the experimental data.

Our results indicate that reasonable estimates for the protein backbone angle ψ in ubiquitin can be made using a simple Karplus equation (Equation 2) for $^1J(N_i,C_{\alpha i})$. It is the simplest model that adequately describes the experimental coupling constants. $^1J(N_i,C_{\alpha i})$ couplings are found to be independent on ϕ and to be weakly dependent on ψ.

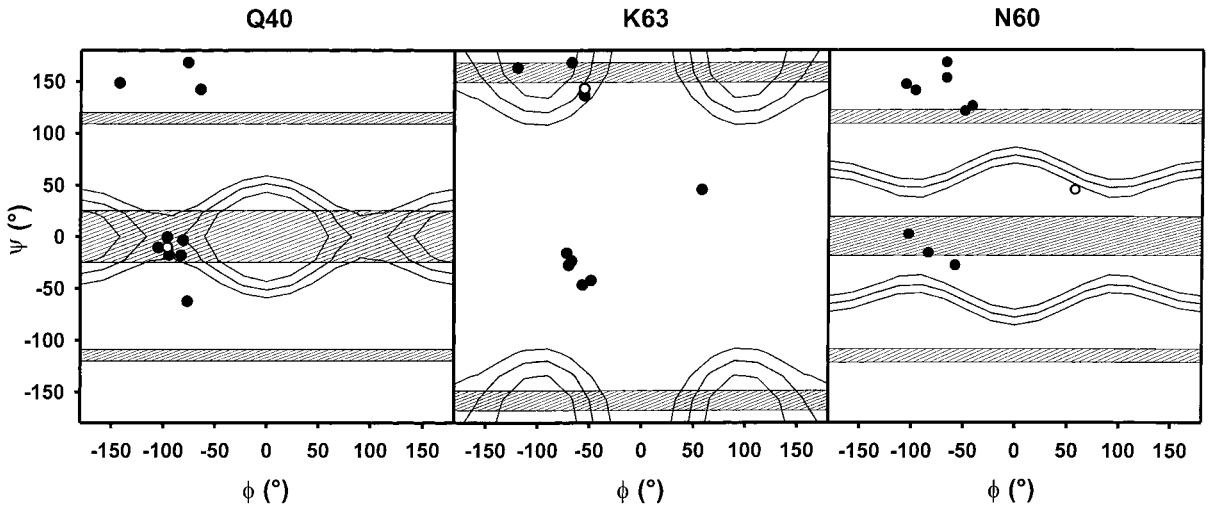

Figure 6. Ramachandran plot showing predicted conformations for Q40, K63 and N60. Open circle presents the conformation in the ubiquitin structure, closed circles present conformations predicted by TALOS. Dashed and grey regions indicate possible conformations calculated from experimental $^1J(N_i,C_{\alpha i})$ and $^2J(N_i,C_{\alpha(i-1)})$ coupling constants, respectively (including an error estimate of ±0.2 Hz which is twice the experimental error).

Analysis of $^2J(N_i, C_{\alpha(i-1)})$ coupling constants

Following Edison et al. (1994a,b), the dependence of 113 coupling constants in ubiquitin and staphylococcal nuclease were investigated. As observed for the $^1J(N_i,C_{\alpha i})$ coupling constants, a direct correlation of $^2J(N_i,C_{\alpha(i-1)})$ with ϕ or $\phi_{(i-1)}$ (both angles were investigated, as two sequential amino acids are involved) cannot be observed, whereas the $^2J(N_i,C_{\alpha(i-1)})$ as a function of $\psi_{(i-1)}$ can be fitted to a functional form given in Equation 2, if ψ is replaced with $\psi_{(i-1)}$ ($R = 0.91$ ($R^2 = 0.82$)). The coefficients are $A = 7.6213$, $B = -1.3791$ and $C = -0.2067$ and the probability that this correlation occurs by chance is negligible ($P < 10^{-4}$) (figure 4B). An equation $f(\phi_{(i-1)},\psi_{(i-1)})$ following Equation 3 was fitted using a least square optimization, yielding $R = 0.94$ ($R^2 = 0.88$). The coefficients describing a surface are $A = 7.8163$, $B = -0.1717$, $C = -0.6408$, $D = -1.3892$ and $E = -0.3709$. Applying F-statistics results in $F = 5.53$ which fulfills the condition that $F > F_{0.01,2,108}$ as $F_{0.01,2,125} = 4.78$, $F_{0.01,2,100} = 4.82$. Therefore the five parameter equation (result of the fit is shown in Figure 5) describes the experimental data better than the Karplus fit, indicating that $^2J(N_i,C_{\alpha(i-1)})$ is not only dependent on $\psi_{(i-1)}$ but also on $\phi_{(i-1)}$.

The correlation coefficient following Edison et al. (1994a,b) for staphylococcal nuclease alone and for the combined data set is $R = 0.79$ ($R^2 = 0.63$).

$^1J(N_i, C_{\alpha i})$ and $^2J(N_i, C_{\alpha(i-1)})$ in denatured ubiquitin

Figure 3 shows the $^1J(N_i,C_{\alpha i})$ and $^2J(N_i,C_{\alpha(i-1)})$ coupling constants in the denatured state of ubiquitin. Uniform coupling constants are observed for denatured ubiquitin ($^1J(N_i,C_{\alpha i}) = 10.9 \pm 0.2$ Hz and $^2J(N_i,C_{\alpha(i-1)}) = 8.0 \pm 0.3$ Hz). Mean values for the individual amino acid range from $^1J(N_i,C_{\alpha i}) = 10.8 \pm 0.2$ Hz for Val, Ile and Leu to $^1J(N_i,C_{\alpha i}) = 11.1 \pm 0.1$ Hz for Asp and Asn residues and from $^2J(N_i,C_{\alpha(i-1)}) = 7.7 \pm 0.2$ Hz for Phe and Ile to $^2J(N_i,C_{\alpha(i-1)}) = 8.2 \pm 0.1$ Hz for Asp, Arg, Val and His residues. The difference between the mean coupling constant values for the individual amino acid is therefore $\Delta^1J(N_i,C_{\alpha i}) = 0.3$ Hz and $\Delta^2J(N_i,C_{\alpha(i-1)}) = 0.5$ Hz. Using the parameterization given in Equation 2 ($f(\psi)$) and Equation 3 ($f(\phi_{i-1},\psi_{i-1})$, mean values for the coupling constants using pairs of ϕ and ψ angles for 85 proteins of the pdb following Smith et al. (1996) were predicted for a protein in the random coil (rc) state: $^1J(N_i,C_{\alpha i})^{rc} = 10.7 \pm 0.2$ Hz and $^2J(N_i,C_{\alpha(i-1)})^{rc} = 7.8 \pm 0.4$ Hz. Thus, the observed coupling constants are in agreement with the model for the random coil state of a protein (Schwalbe et al., 1997; Smith et al., 1996; Hennig et al., 1999; Peti et al., 2000).

Discussion

Parameterizations for the dependence of $^1J(N_i,C_{\alpha i})$ and $^2J(N_i,C_{\alpha(i-1)})$ coupling constants on the protein backbone angles were derived. It was shown that these parameterizations can be applied successfully to predict coupling constants in the random coil state of proteins. It is not possible to derive a single pair of protein backbone angles from measured $^1J(N_i,C_{\alpha i})$ and $^2J(N_i,C_{\alpha(i-1)})$ coupling constants. However, it is possible to differentiate between different secondary structure elements. Furthermore, $^1J(N_i,C_{\alpha i})$ and $^2J(N_i,C_{\alpha(i-1)})$ coupling constants were found to be a useful tool in cases of ambiguous predictions from TALOS (Cornilescu et al., 1999) as discussed below:

Using TALOS, 55 ϕ/ψ good angle predictions for ubiquitin can be derived. In the following, predictions derived by TALOS from the dataset of ubiquitin were excluded. For 19 residues in ubiquitin, TALOS does not provide an unambiguous prediction. In this report, $^1J(N_i,C_{\alpha i})$ and $^2J(N_i,C_{\alpha(i-1)})$ coupling constants were measured for 9/8 of these 19 residues. Figure 6 shows the obtained angle pairs of ϕ and ψ from the TALOS prediction and the correct values for ϕ and ψ in the ubiquitin structure for the residues Q40, K63 and N60. Using coupling constant data, the derived ϕ and ψ angles for Q40 ($\phi = -92 \pm 9°$ and $\psi = -10 \pm 7°$) are in good agreement with the backbone angles in the ubiquitin structure: $\phi = -96°$ and $\psi = -10°$. For K63, TALOS predicts pairs of ϕ and ψ in two clustered regions of the Ramachandran diagram. Comparison with prediction from coupling constants selects the region from the Ramachandran diagram ($\phi = -80 \pm 34°$ and $\psi = 155 \pm 17°$), which is in agreement with the structural data ($\phi = -50°$ and $\psi = 143°$). For all other residues but N60, similar results are obtained. None of the TALOS predicted ϕ/ψ pairs is in agreement with the actual conformation of N60 in the ubiquitin structure. In contrast, the prediction made from $^2J(N_i,C_{\alpha(i-1)})_{I61}$ and $^1J(N_i,C_{\alpha i})_{N60}$ do not exclude the correct conformation in the α_L region of the Ramachandran diagram. Thus, the use of $^2J(N_i,C_{\alpha(i-1)})$ coupling constants in combination with TALOS can clarify the few ambiguous predictions from TALOS based on chemical shifts.

Conclusions

A new method to measure $^1J(N_i,C_{\alpha i})$ and $^2J(N_i,C_{\alpha(i-1)})$ coupling constants in folded and unfolded proteins was introduced. The method is based on a J-modulated sensitivity enhanced HSQC and is therefore easy to implement and useful in systems with limited chemical shift resolution such as denatured proteins.

Measured $^2J(N_i,C_{\alpha(i-1)})$ coupling constants were found to be a valuable indicator to identify secondary structure elements in folded proteins. Under the premise that the backbone torsion angle ω is restricted to *trans* ($\omega \approx 180°$), the dependence on protein backbone torsion angle conformations was quantified, and it was shown, that simple models describe the observed coupling constants well. $^2J(N_i,C_{\alpha(i-1)})$ is correlated with the torsion angles $\phi_{(i-1)}$ and $\psi_{(i-1)}$. Coupling constants in the denatured state of ubiquitin were found to be uniform along the sequence of the protein and independent of a given residue type. Furthermore it was shown, that the mean coupling constant is in good agreement with predicted coupling constants using the random coil theory.

The ease of access make $^1J(N_i,C_{\alpha i})$ and $^2J(N_i,C_{\alpha(i-1)})$ coupling constants an interesting parameter, together with chemical shift data (Cornilescu et al., 1999) for the rapid identification of secondary structure elements in proteins.

Acknowledgements

We thank the Massachusetts Institute of Technology (Start-up funds and Rosenblith stipend), the Karl Winnacker-Foundation, the Fonds der Chemischen Industrie and the BMBF, the DFG (Schw701/3-1), the LSF for Biomolecular NMR (HPRI-1999-CT-00014) and the RTD project FIND STRUCTURE (HPRI-CT-1999-40005) for financial support.

References

Bax, A., Vuister, G.W., Grzesiek, S., Delaglio, F., Wang, A.C., Tschudin, R. and Zhu, G. (1994) *Meth. Enzymol.*, **239**, 79–105.

Bevington, P.R. (1969) In *Data reduction and Error Analysis for the Physical Sciences*, McGraw-Hill, New York, NY, pp. 195–203.

Billeter, M., Neri, D., Otting, G., Qian, Y.Q. and Wüthrich, K. (1992) *J. Biomol. NMR*, **2**, 257–274.

Bronstein, I.N. and Semendjajew, K.A. (1989) In *Taschenbuch der Mathematik*, 24th edn., Verlag Harri Deutsch, Thun & Frankfurt/M., pp. 24–27.

Bystrov, V.P. (1976) *Prog. NMR Spectrosc.*, **10**, 44–81.

Cornilescu, G., Delaglio, F. and Bax, A. (1999) *J. Biomol. NMR*, **13**, 289–302.

Cornilescu, G., Marquardt, J.L., Ottiger, M. and Bax, A (1998) *J. Am. Chem. Soc.*, **120**, 6836–6837.

Delaglio, F., Torchia, D.A. and Bax, A. (1991) *J. Biomol. NMR*, **1**, 439–466.

Edison, A.S., Markley, J.L. and Weinhold, F. (1994a) *J. Biomol. NMR*, **4**, 519–542.
Edison, A.S., Weinhold, F., Westler, W.M., and Markley, J.L. (1994b) *J. Biomol. NMR*, **4**, 543–551.
Emsley, L. and Bodenhausen, G. (1990) *Chem. Phys. Lett.*, **165**, 469–476.
Heikkinenen, S., Permi, P. and Kilpeläinen, I. (2001) *J. Magn. Reson.*, **148**, 53–60.
Hennig, M., Bermel, W., Schwalbe, H. and Griesinger, C. (2000) *J. Am. Chem. Soc.*, **122**, 6268–6277.
Hennig, M., Bermel, W., Spencer, A., Dobson, C.M., Smith, L.J. and Schwalbe, H. (1999) *J. Mol. Biol.*, **288**, 705–723.
Juranić, N. and Macura, S. (2001) *J. Am. Chem. Soc.*, **123**, 4099–4100.
Kay, L.E., Ikura, M., Tschudin, A. and Bax, A. (1991) *J. Magn. Reson*., **89**, 496–514.
Kuboniwa, H., Grzesiek, S., Delaglio, F. and Bax, A. (1994) *J. Biomol. NMR*, **4**, 871–878.
Konradi, R., Billeter, M. and Wüthrich, K. (1996) *J. Mol. Graphics*, **14**, 52–55.
Loll, P.J. and Lattman, E.E. (1989) *Proteins*, **5**, 183–201.
Meissner, A., Duus, J.Ø. and Sørensen O.W. (1997) *J. Biomol. NMR*, **10**, 89–94.
Neri, D., Otting, G. and Wüthrich, K. (1990) *J. Am. Chem. Soc.*, **112**, 3663–3665.
Mierke, D.F., Gradolnik, S.G. and Kessler, H. (1992) *J. Am. Chem. Soc*., **114**, 8283–8284.
Permi, P. and Annila, A. (2000) *J. Biomol. NMR*, **16**, 221–227.
Permi, P., Rosevar, P.R. and Annila, A. (2000) *J. Biomol. NMR*, **17**, 43–54.
Peti, W., Hennig, M., Smith, L.J. and Schwalbe, H. (2000) *J. Am. Chem. Soc.*, **122**, 12017–12018.
Peti, W., Smith, L.J., Redfield, C. and Schwalbe, H. (2001) *J. Biomol. NMR*, **19**, 153–165.
Schwalbe, H., Fiebig, K.M., Buck, M., Jones, J.A., Grimshaw, S.B., Glaser, S.J., Smith, L.J. and Dobson, C.M. (1997) *Biochemistry*, **36**, 8977–8991.
Shaka, A.J., Barker P.B. and Freeman, R. (1985) *J. Magn. Reson.*, **64**, 547–552.
Smith, L.J., Bolin, K.A., Schwalbe, H., MacArthur, M.W., Thornton, J.M. and Dobson, C.M. (1996) *J. Mol. Biol.*, **255**, 494–506.
Tjandra, N. and Bax, A. (1997) *J. Magn. Reson.*, **124**, 512–515.
Tjandra, N., Grzesiek, S. and Bax, A. (1996) *J. Am. Chem. Soc.*, **118**, 6264–6272.
Vuister, G.W., Delaglio, F. and Bax, A. (1993) *J. Biomol. NMR*, **3**, 67–80.
Wang, A.C., Grzesiek, S., Tschudin, R., Lodi, P.J. and Bax, A. (1995) *J. Biomol. NMR*, **5**, 376–382.